Schweizerische Eidgenossenschaft
Confédération suisse
Confederazione Svizzera
Confederaziun svizra

Eidgenössisches Departement des Innern EDI
Bundesamt für Meteorologie und Klimatologie MeteoSchweiz

Arbeitsbericht MeteoSchweiz Nr. 230

Experimental investigation of micrometeorological influences on birch pollen emission

D. Michel, M.W. Rotach, R. Gehrig, R. Vogt

Arbeitsbericht MeteoSchweiz Nr. 230

Experimental investigation of micrometeorological influences on birch pollen emission

D. Michel[1,2], M.W. Rotach[1,3], R. Gehrig[1], R. Vogt[2]

[1] Federal Office of Meteorology and Climatology MeteoSwiss
[2] Institute of Meteorology, Climatology and Remote Sensing, University of Basel
[3] present affiliation: Institute of Meteorology and Geophysics, University of Innsbruck, Austria

Bitte zitieren Sie diesen Arbeitsbericht folgendermassen
Michel, D, MW Rotach, R Gehrig, R Vogt: 2010, Experimental investigation of micrometeorological influences on birch pollen emission, *Arbeitsberichte der MeteoSchweiz*, **230**, 37 pp.

Herausgeber
Bundesamt für Meteorologie und Klimatologie, MeteoSchweiz, © 2010

MeteoSchweiz
Krähbühlstrasse 58
CH-8044 Zürich
T +41 44 256 91 11
www.meteoschweiz.ch

Weitere Standorte
CH-8058 Zürich-Flughafen
CH-6605 Locarno Monti
CH-1211 Genève 2
CH-1530 Payerne

Acknowledgments

Our great appreciation goes to the European Cooperation in Science and Technology (COST) Action ES0603, which allowed us to conduct this project in the first place. The financial support for this project by the State Secretariat for Education and Research, SBF, grant C07.0111, is gratefully acknowledged. Many thanks go to the staff at MeteoSwiss Zurich and Payerne and the MCR Lab, University of Basel. Their contribution to the field campaign and the pollen analysis is very appreciated. Without their help, this study could never have been performed.

Our special thanks go to Ambros Werner from the MCR Lab and Benoît Guillod from MeteoSwiss. They supported us during the entire campaign and made that time very enjoyable. I also want to express my gratitude to Paul Kunz who kindly allowed me to use large areas of his property for the instrumental set-up and his patience during the entire campaign period.

Zurich, June 21, 2010

Contents

List of Figures

List of Tables

1 Introduction

Diseases due to aeroallergens increased over the last decades and affect more and more people. The overall prevalence of seasonal allergic rhinitis in Europe is about 15 precent and increasing. Adequate protective and pre-emptive measures require both the reliable assessment of production and release of various pollen species, and the forecasting of their atmospheric dispersion. A new generation of pollen forecast models, which may be either based on statistical knowledge or full physical transport and dispersion modeling, can provide pollen forecasts with full spatial coverage (Ambelas Skjøth et al., 2006; Helbig et al., 2004; Schueler and Schlünzen, 2006; Sofiev et al., 2006a,b). Such models are currently being developed in many European countries. Basically, the central part of these recent pollen forecast models corresponds to traditional air pollution transport and dispersion models (Venkatram and Wyyngaard, 1988). The main difference between traditional air pollutants and pollen consists of the fact that the latter are heavy and thus subject to gravitational forces. The most important shortcoming in these pollen dispersion systems is the description of the emissions. This is largely due to the missing knowledge in the physical and biological processes that determine emissions, namely the dependence of the emission rate on physical processes such as turbulent exchange or mean transport and biological processes such as ripening and preparedness for release. Thus the quantification of the pollen emission and determination of the governing synoptic and micrometeorological factors are subject of the present project *MicroPoem*, which includes experimental field work as well as numerical modeling. The overall goal of the project is to derive an emission parameterization based on meteorological parameters, eventually leading to enhanced pollen forecast models.
Within the COST Action ES0603 (*EUPOL*), which is dedicated to the assessment of production, release distribution and health impact of allergenic pollen in Europe, one working group focuses on pollen production and release and their quantitative description. It includes analysis of observational and modeling information for revealing key characteristcs of these processes. From this framework the project *MicroPoem* emerged as a collaboration of the Federal Office of Meteorology and Climatology MeteoSwiss and the Institute of Meteorology, Climatology and Remote Sensing at the University of Basel, Switzerland.
The overall goal of the current research is investigating pollen production and emission by combining experimental and modeling work in order to quantify the released pollen as function of meteorological parameters. As an example, birch trees are used because their pollen are among the most important allergens in Europe. Micrometeorological analyses focus on reproducing the observed downwind pollen distribution by using a local dispersion model. The micrometeorological observations will thereby yield the necessary input of turbulence characteristics. The goal is to derive an emission parameterization based on meteorological variables. The new emission parameters will be tested by applying them in an operational pollen dispersion model.

1.1 State of research

Several studies on the impact of meteorological factors on pollen concentration, emission and dispersion have been published, of which some included modeling and/or experimental work. In the context of diseases due to aeroallergens in Europe Nieddu et al. (1997) investigated the intensity and timing of olive pollination in relation to phenological stages and the influence of meteorological parameters on pollen emission and dispersal. They found a significant positive correlation between pollen concentrations and hourly air temperature and a negative correlation between pollen concentrations and air humidity. These findings were confirmed by Méndez et al. (2005), who measured airborne birch pollen and several meteorological parameters between 1992 and 2000. A positive correlation between pollen count and both temperature and shortwave downward radiation and a negative correlation for relative humidity were observed. They conclude that air temperature is the determining factor for flowering onset and intensity. A predictive model for the calculation of the total annual airborne olive pollen output on the basis of a set of meteorological and pollen data is described by Galán et al. (2001). The results indicated an agreement of less than 10 % between modeled and observed data.
In the last decade in particular the extensive adoption of genetically modified crops has led to the need to better understand the pollen dispersion in the atmosphere because of the potential for unwanted movement of genetic characteristics via pollen transport. Lavigne et al. (1998) performed a pollen-dispersal experiment in the framework of the assessment of gene flow associated with the release of transgenic oilseed rape (Lavigne et al., 1996). Brunet et al. (2004) investigated the presence of viable maize pollen within the Boundary Layer as an evidence for long-range transport. At all heights pollen concentrations of the order of concentrations near the ground were observed. They also found that maize pollen seem to behave like a gas or small particles, since their settling velocity is small compared to the vertical velocities found in the Convective Boundary Layer. Aylor et al. (2006) and Boehm et al. (2008) assessed the agreement between horizontal and vertical profile measurements of maize pollen concentrations and the results of a Lagrangian stochastic model. Chamecki et al. (2009) validated Large Eddy Simulations of pollen dispersal with experimental data of pollen emission and downwind deposition. They conclude that the main parameter governing the shape of the dispersion is the turbulent transport and the ratio between settling of the pollen due to the gravitational effect.
In the field of agroecology several experiments and modeling works on the concentration and aerial transport of fungal species causing foliar disease have been performed at the Computational Epidemiology and Aerobiology Laboratory (CEAL) at Pennsylvania State University (Isard et al., 2007; Magarey and Isard, 2005).
In terms of investigating plant reproduction and dispersion Raynor et al. (1970) performed a study on the correlation of meteorological factors to the dispersion and deposition of ragweed pollen released both naturally and artificially. They conclude that the variation of pollen dispersion and deposition rates is regulated not only by meteorological but both biological and meteorological factors. Van Hout et al. (2008) performed field experiments including vertical profile measurements to study the diurnal cycle of corn pollen immission and its relation to meteorological and mic-

rometeorological conditions. They found a strong decrease of pollen concentrations with increasing height. The diurnal cycles of pollen concentrations were characterized as uni-modal or bi-modal with peak values during the morning and decreasing values during the afternoon. They conclude that humidity and solar radiation may be important variables that govern the release of pollen. They also found a correlation of high pollen concentration periods to ejection periods in coherent structures within the Canopy Boundary Layer. The behavior of different airborne pollen concentrations at different heights in relation to meteorological factors was studied by Comtois et al. (2000). They found evidence for a layer of pollen transport at about 500 m above the ground with pollen concentrations higher by 30 % compared to ground level.

Concerning its goal and set-up, the experiment presented here is unique and ambitious. The obtained meteorological and micrometeorological data allow to describe the characteristics of the local-scale conditions around the pollen source. The pollen counts, however, indicate a significant variability due to several errors incorporated in pollen sampling methods. The calibration of pollen counts, therefore, is necessary prior to the assessment of the influence of meteorological and micrometeorological factors on pollen concentrations.
The present report aims at describing in detail the experimental work performed in the field in spring 2009, and at summarizing all the instrumentation and necessary post-processing of the data (Section 3). Data availability is laid out in Section 4, while Section 5 provides a first assessment of the meteorological data as well as the plausibility of the pollen measurements.

2 Aim and outline of the experiment

Since pollen are difficult to emit in a controlled fashion, as in tracer experiments for 'ordinary' pollutants, the experimental set-up will have to respond to the need of inferring the emission from the observed downwind concentrations (a typical inversion problem). In order to have a well-defined source location, an isolated group of birch trees has been chosen. To facilitate the measurements, the experiment location has been chosen such that it is dominated by two main wind directions, which is usually the case in a valley.
The experimental set-up aimed at measuring the exchange conditions in a longitudinal transect. This consisted of vertical upwind and downwind profile measurements at four locations using sonic anemometers and a sound detecting and ranging system (SODAR) as well as a tethered balloon sonde. Auxiliary measurements of all relevant meteorological elements have been carried out during the campaign at a separate tower. Simultaneously, the pollen concentration was probed using several pollen traps of four different types. Basically, the approach was to determine pollen concentrations downwind of the source, with reference (background concentration) measurements upwind of the source. A large number of traps was distributed hori-

zontally, i.e. longitudinal and in cross-wind direction, as well as vertically (mounted on the micrometeorological profile towers and on the balloon tether). The horizontally distributed pollen traps were only operated during intensive operation periods (IOPs) with a temporal resolution of one hour averages. The vertical pollen concentration profile was probed continuously at three locations with a temporal resolution of two hours.
Eventually, it is assumed that these measurements provide enough information to determine the emission from the observed downwind concentrations using a three-dimensional Lagrangian stochastic particle model. With the actual emission being estimated, a parameterization can be derived from the observed meteorological data. In forecast models, such as the COSMO-ART[1], the acquired emission parameter will then replace the set of functions currently used, which provide a probable rather than accurate emission potential. The current functions contain empirically weighted parameters such as shear stress velocity and heat-sum coefficients.
An important weakness of large-scale forecast applications that is not addressed by the current research, however, is the missing knowledge of the spatial source distribution along the modeled trajectories.

3 Description of the experiment

Experimental data have been collected in a large field campaign, which has been conducted in Illarsaz, Switzerland in April 2009. The start of the measurements was determined by applying a time of flowering prediction model based on growing degree days (GDD). The set-up was designed to derive the emission from the observed downwind concentrations of a well-defined pollen source. Pollen concentrations and meteorological factors have been measured at locations upwind and downwind of a pollen source at a high spatial and temporal resolution. Key features of the set-up were the horizontal as well as vertical profile measurements of pollen concentrations and (micro-)meteorological conditions. In order to have a well-defined source location, an isolated group of birch trees has been chosen, which was located in a valley floor. This condition allowed to presume a rather persistent wind direction and considerable velocity during day- and nighttime. The measurements provided a dataset covering twenty days with a large array of variables. These included both continuous and discontinuous pollen concentration measurements, as well as continuous meteorological information.

[1]COSMO (COnsortium for Small-scale MOdeling) was originally developed at the German Weather Service (DWD) (Doms and Schaettler, 2002) and further developed in the framework of COSMO to COSMO-*ART* (Artificial and Reactive Tracer gases). The latter is currently evaluated for operational use at the Federal Office for Meteorology and Climatology MeteoSwiss.

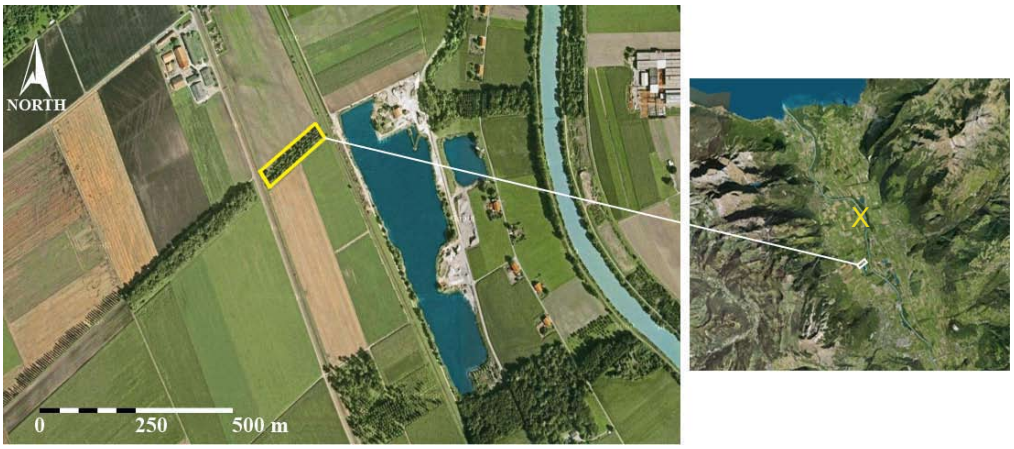

Figure 3.1: Satellite image of the experiment location at Illarsaz (Valais), Switzerland. The source location is indicated with the yellow (left) and white (right) rectangle. The image on the right shows the exposition of the valley and the terrain. The yellow cross denotes the location of the SwissMetNet station. The image was taken March 5 , 1997.

3.1 Location and surrounding area

The search of the experiment location was guided by preliminary assumptions on most favorable sites for obtaining reliable and effective measurements: First, the pollen source should consist of a considerable number of grouped and isolated (with respect to other species) adult birch trees. Following this assumption, the footprint of the measured pollen concentration is well-defined. Second, the fetch area upwind as well as downwind of the source should be of at least several hundred meters length and free of obstacles. Thus, a more or less homogeneous pollen concentration distribution as well as turbulent structure will be advected past the sensors. Third, the source should stand within a valley, where diurnal upvalley winds and nocturnal downvalley winds occur.
The latter two phenomena are components of the mountain-plains wind system, which is characterised by a cycle of local daytime upvalley (from plains) winds and nighttime downvalley (from mountain) winds near the surface (Steinacker, 1984; Weigel et al., 2006). It usually occurs during clear periods with high solar irradiance and weak synoptic flow. Among others, the geometry of a mountain valley effects that the same irradiated area corresponds to a much smaller volume of air compared to the situation over adjacent plains. The atmosphere in the valley is, therefore, heated stronger during daytime and cooling faster during nighttime compared to the air above the plains. These resulting temperature gradients between plains and valley cause a cyclic wind system with a diurnal pattern. During daytime air from the plains flows into the valley and air from the valley flows back into the plains during nighttime. A return branch at higher elevation is sometimes present, flowing in the direction opposite the surface winds and completing the circulation.
The occurrence of a mountain-plains wind system determined the set-up orientation due to persistent wind directions during the upvalley and downvalley wind phases. Furthermore, diurnal *and* nocturnal downwind measurements of pollen concentra-

tion and turbulence are possible with the same sensors, since the wind direction changes about 180 degrees within a mountain-valley wind system cycle.
A corresponding location was found in Illarsaz in the canton Valais, Switzerland at 385 m a.s.l (46°17' N 6°55' E, Fig. 3.1). It lies centrally within the valley of the Rhone river, which in this region extends in a northwesterly to southeasterly direction and is approximately 5.7 km wide. The valley opens to the Northwest, where it reaches the Lake of Geneva at approximately 11.5 km from the experiment location. To the South the valley narrows to about 1.5 km in width approximately 12 km from the source. The predominant landuse in this region is agricultural. During daytime a northwesterly valley wind was expected to prevail, which was altogether confirmed by the measurements (see Section 5.1). It was, however, sometimes superimposed by the south foehn wind flowing over the Alps. Yet in general, the valley wind was rather strong due to the large area being irradiated and hence was seldom superimposed by synoptic systems. The observations of the downvalley wind showed lower velocities and smaller variance than its daytime correspondence.

3.1.1 Pollen source

The pollen source (Fig. 3.2) consists of two different birch species, *Betula pubescens* (larger fraction) and *Betula pendula*, of which both were considered equally in the experiment. The birch trees were all of 17-22 m height. It consists of approximately 140 birch trees and around 50 individuals of various species, such as spruce, scots pine, ash and oak. The crop is approximately 200 m wide in the cross-wind direction and 40 m in the longitudinal direction. The source is, therefore, considered a line-source rather than a point-source. This instance lead to a number of consequences on the part of the assumed dispersion pattern and hence the set-up (see Section 3.2). The below-average number of catkins carried by individuals in this birch plot suggests that the vitality of the birch trees is mediocre. The largest part of the catkins was carried in the treetops or at least in the upper half of the trees. Thus, on the one hand a potentially below-average absolute pollen emission was expected, and on the other hand the duration of the emission period was presumed to be shorter than typical, i.e. less than four weeks (Gehrig pers. comm.). The emission potential of the source will be estimated on the basis of manual countings of the catkins, which will yield an approximate guidance level for the modeled emission. The understorey of the plantation mostly consists of grass of 0.3 to 0.5 m height.

3.1.2 Up- and downwind area

The pollen source was located between two agricultural fields in the longitudinal direction and bordered in the cross-wind direction perpendicularly by a train track in the east and a country street as well as an industrial canal in the west (Fig. 3.1). The agricultural field in the north, i.e. the daytime upwind fetch, was a fallow throughout the experiment period and is of 475 m length. The diurnal downwind area in the south was partitioned centrally into a pasture field in the east and a potato crop in the west. The undisturbed downwind area is about 500 m long and limited by a cottonwood plantation. The pasture height was 0.15 m at the beginning and reached a maximum of 0.3 m at the end of the experiment. The potato

crop represents a rather special case: It was completely covered with acryl sheets for insulation. Hence, the surface roughness is assumed to change significantly the in cross-wind direction.
The sourrounding area is scarcely populated and dominated by agricultural plains, as mentioned earlier. The crop areas are commonly bordered by cross-wind orientated tree-lines, which are accounted for the most important elements creating wind shear in the Roughness Sublayer. These tree-lines consist of several species (such as mentioned in Section 3.1.1), among which in the northern region a rather large number of birch trees were found. The diurnal upwind area is hence interspersed with trees contributing to the background birch pollen concentration. The closest birch-populated tree-lines were found at a distance of approximately 600 m from the main source. A precaution for considering the influence of these sources was the characterization of the background concentration level during the experimental period.
Agriculture being the predominant landuse, airborne dust due to heavy-vehicle traffic and dispersal of herbicides were considerable factors in terms of pollen sampling, since all additional trapped objects impede reliable counting.

3.2 Materials and methods

The set-up basically consisted of vertical and horizontal profile measurements. The vertical profiles have been aligned in the longitudinal direction of the valley and provided pollen concentration as well as turbulence data. An array of horizontally aligned traps measured pollen concentration profiles in the longitudinal and the cross-wind direction. The arrangement of the instruments, most important the longitudinal distance from the source, has been determined by applying a Lagrangian particle dispersion model (Rotach et al., 1996; De Haan and Rotach, 1998), using a set of probable input parameters. The model results should ensure that the peak of downwind pollen concentrations lies within the range covered by the instrumental array and not beyond it even at higher wind velocities (see Section 5).
Beside data quality, the success of the experiment mainly depended on the statistically significant quantity of sampled pollen. In contrast to meteorological and micrometeorological measurements, pollen sampling methods rely, in most cases, on manual counting. Automatic optical instruments in the stage of evaluation are described by Takahashi et al. (2001); Masanari and Tadashi (2003); Shigeto et al. (2004); Shigetoshi et al. (2005) and Ronneberger (2007). In the current work the large number of pollen samplers implies time-consuming counting work. Therefore, the experimental period was divided into two operating schemes (note that regardless of the current scheme, meteorological and micrometeorological data were measured continuously):

- **routine operation:** Burkard and Burkard Scientific (Sc.) samplers (see Section 3.2.3) were operated in the Seven Days Mode.

- **intensive operation:** Burkard samplers were operated as above. Burkard Sc. were operated in the 24 hours Mode; additional pollen samplers (see Section 3.2.3) were operated.

Figure 3.2: Picture of the profile tower 100 m south of the main pollen source (visible in the background).

Table 3.1: Tower instrumentation.

instrument	height a.g.	resolution	instrument	height a.g.	resolution
T_1			T_2		
CSAT3	1.8 m	20 Hz	CSAT3	1.9 m	20 Hz
CSAT3	8.9 m	20 Hz	CSAT3	4.4 m	20 Hz
CSAT3	17.8 m	20 Hz	CSAT3	9.0 m	20 Hz
Burkard	2 m	2 h	CSAT3	13.5 m	20 Hz
Burkard	18 m	2 h	CSAT3	18.0 m	20 Hz
T_3			Burkard Sc.	2 m	1/2 h
CSAT3	2.0 m	10/20 Hz	Burkard Sc	18 m	1/2 h
CSAT3	9.0 m	10/20 Hz	Psychr. I	2 m	1 min
CSAT3	18.0 m	10/20 Hz	Psychr. II	6 m	1 min
Burkard	2 m	2 h			
Burkard	18 m	2 h			

During the experimental period six IOPs have been conducted during fair weather days to ensure pollen release and upvalley wind. See Fig. 5.1 for the dates when IOPs have been conducted.

3.2.1 Profile measurements of micrometeorological parameters and pollen concentrations

The vertical atmospheric profile was monitored at three towers of 18 m height each, which corresponds approximately to the average canopy height of the pollen source (Fig. 3.3) and the lower part of the Roughness Sublayer. They were located 30 m north (T_1), 100 m south (T_2) and 350 m south (T_3) of the main pollen source and their instrumentation was the same in principle. They were equipped with CSAT3 ultrasonic anemometers (Campbell Scientific Ltd.) and a Burkard pollen sampler on top (for the individiual instrument mounting height see Table 3.1). The mounting of the Burkard sampler at this height above the ground was an outstanding feature of this campaign, since profile measurements using this sampling method are unique to date. Next to each tower a Burkard pollen sampler was set up at 2 m above the ground. CR1000 data loggers (Campbell Scientific Ltd.) were used at the towers T_1 and T_3 and a CR3000 (Campbell Scientific Ltd.) at T_2. T_1 was equipped with three ultrasonic anemometers and measured the diurnal background birch pollen concentration and upwind turbulence. These measurements were crucial because of

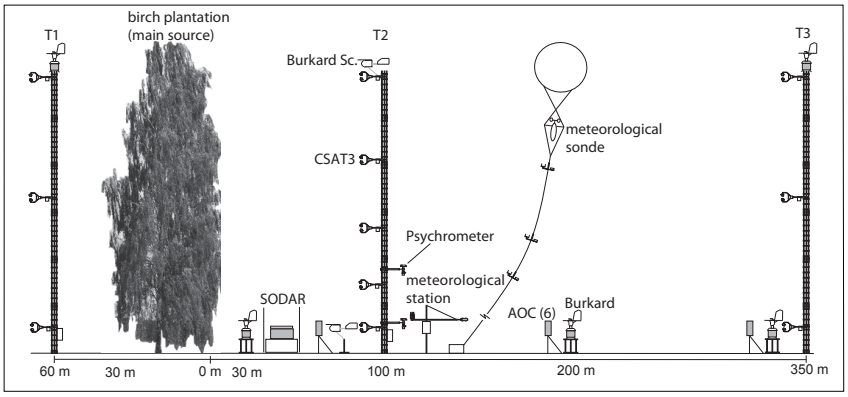

Figure 3.3: Longitudinal section of the experimental set-up. The indexed T's denote the profile tower number mentioned in the text.

the considerable number of birch trees in the surrounding area, and because they served as reference. South of the main pollen source T_2 and T_3 measured the diurnal downwind concentration and turbulence. T_2 was equipped with five ultrasonic anemometers and a Burkard Sc. (Fig. 3.2). The higher vertical resolution of turbulence makes it the principal station for diurnal turbulence characteristics downwind of the source. T_3 was equipped in the same way as T_1.
The temporal resolution of the ultrasonic anemometers was 20 Hz for turbulence measurements during most of the experimental period (see Section 4) and 30 minutes for the calculated fluxes. The Burkard samplers allow a maximum temporal resolution of one hour, which implies a relatively high uncertainty in the results. Thus, the applied temporal resolution used was two hours, which is more accurate. The two Burkard Sc. samplers used at T_2 allow an accurate resolution of one hour or two hours depending on the operation mode (Section 3.2.3).
The horizontal pollen concentration profile was monitored with an array of 18 Air-O-Cell (AOC) traps (Zefon International) mounted at 2 m above the ground. The grid-based set-up of pollen samplers is a further feature of the campaign, since it leads to a unique data set of spatially highly resolved ground pollen concentrations. The array consisted of three cross-wind aligned rows with six AOCs each (Fig. 3.4). Rather than a arcwise set-up, which one would choose for a point source, this rectangular alignement has been chosen. In a first approach it was assumed that the emission and transport of the pollen concentration is more or less homogeneous in the lateral direction. The distance between the AOCs in the lateral direction was 30 to 44 m in every column. The cross-wind width of the AOC array approximately corresponded to the width of the main pollen source only, since the terrain did not allow for extension in the lateral direction.

The AOCs were operated each IOP from 07:00 to 15:00 UTC+1 in the shortest and to 18:00 in the longest measurement period. The desired temporal resolution was one hour. The manual hourly exchange routine of AOC cassettes was, however, rather time-consuming because of the large number of sensors and the long walking distances in between. Thus, a sampling period of 45 minutes was chosen which

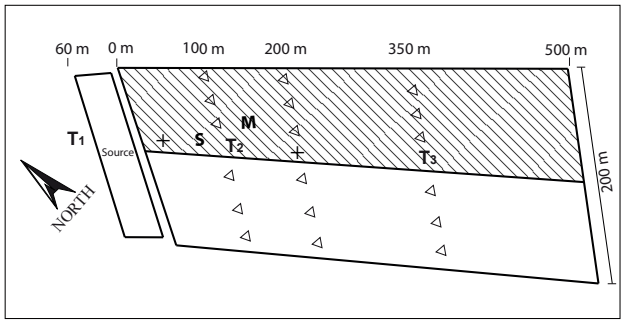

Figure 3.4: Top view of the experimental set-up. The hatched area denotes the pasture crop, the large plain denotes the potato crop covered with acryl sheets. The indexed T's denote the location of the profile towers, the plus signs denote singular Burkard samplers on the ground, S denotes the location of the SODAR, M denotes the location of the meteorological station and the triangles denote AOCs.

left 15 minutes for the entire exchanging process, during which all samplers were switched off. The AOC data were extrapolated to provide hourly resolution.
Another important feature of the campaign is the pollen profile measurement conducted during the IOPs using a tethered balloon. Rotorod pollen samplers (Section 3.2.3) were mounted on the balloon tether in order to reach the measuring heights of 25, 100 and 290 m, respectively, above the ground, when the balloon itself ascended to a maximal height of 300 m. Yet the actual measurement height depended on the decline of the tether. Hence, the heights were smaller during strong wind periods. The real height above the ground was estimated via the measured air pressure gradient between the balloon height and the meteorological station.

3.2.2 Meteorological measurements

Meteorological data, such as long- and shortwave irradiance, wind direction and velocity, soil temperature, soil heat flux and precipitation have been measured continuously at a separate small tower within the area south of the main pollen source near the profile tower T_2 (Fig. 3.5). For the net radiation components a CNR1 net radiometer (Kipp & Zonen) was used without ventilation and heating and operated in the Four Separate Components Mode. Wind direction and velocity, humidity, temperature and pressure as well as precipitation and intensity were measured with a WXT510 weather transmitter (Vaisala Ltd). The soil temperature and the soil heat flux were measured using three CS107 probes (Campbell Scientific Ltd.) and three HF3 heat flux plates (McVan Instruments Inc.), respectively. A CR5000 data logger (Campbell Scientific Ltd.) was used at this station. Two psychrometers were mounted in two different heights (2 and 6 m) on the profile tower, providing air temperature and humidity profiles, allowing to estimate the latent heat flux λE via the Bowen ratio method.
Fifty-eight meters south of the main pollen source a FAS Series SODAR (Scintec AG) was measuring the vertical wind profile (direction and velocity) of the lowest 600 m of the Planetary Boundary Layer. Additionally, a tethered balloon sonde provided vertical profile information on dry and wet temperature, air pressure, wind

Figure 3.5: Picture of the meteorological station. On the right hand side the non-ventilated CNR1 net radiometer is mounted at 2 m above the ground. On the left hand side a WXT510 weather transmitter was mounted. The CS107 soil temperature probes and HF3 heat flux plates are buried around the foot of the station.

direction and velocity during the IOPs.
In this section only the pollen traps are discussed in detail. For information on some of the used micrometeorological instruments and methods, see Arya (2001); Foken (2008); Kaimal and Finnigan (1994); Lee (2004); Michel et al. (2008); Stull (1988); Vogt (1995). For a list of the used instruments see Tables 3.1 and 3.2.

3.2.3 Pollen sampling methods

Table 3.2: Pollen samplers and meteorological instruments.

instrument	height a.g.	temp. resoultion
pollen sampler		
AOC (18)	2 m	1 h
Rotorod	25 m	1 h
Rotorod	100 m	1 h
Rotorod	290 m	1 h
meteorol. station		
WXT	2 m	1 min
CNR1	2 m	1 min
CS107 (3)	-0.02 m	1 min
HF3 (3)	-0.04 m	1 min

Burkard pollen samplers

The Hirst-type pollen traps (Hirst, 1952) used in this experiment are volumetric Burkard samplers (Burkard Scientific Ltd.) of the first and second generation (Mandrioli et al., 1998). The first generation Burkard sampler (Fig. 3.6) is widely used and often serves as the standard pollen sampling method. The cylindrical body of the Burkard basically consists of a pivoted upper and a fixed lower part. Through a horizontally aligned horizontal slot orifice in the upper part, an electric air pump

located in the lower part draws air past a cylinder. The cylinder is rotated on a horizontal axis by a spring-driven clockwork. An air flow rate of 10 l/min is required to enable sampling a large spectrum of pollen species, i.e. from small to larger particle sizes.

Figure 3.6: Burkard pollen sampler mounted on the towertop north of the pollen source.

Figure 3.7: Burkard Sc. mounted on the towertop south of the pollen source with the CSAT3 ultrasonic anemometer in the background.

The orifice is facing oncoming wind by means of a windvane attached to the pivoted upper part. Due to inertia, air suspended particles accelerated by the suction collide with a silicone-coated synthetic strip attached to the cylinder instead of following the air flow through the device (impaction filter). The rotation rate of the cylinder is typically one rotation per seven days and determines the temporal sampling resolution. The second generation of Burkard pollen traps (Burkard Sc., Fig. 3.7) works according to the same principle and with the same air flow rate. Yet it has the advantage of being much smaller and lighter and features an electronic control which allows adjustment of the temporal resolution by changing the rotation rate of the sampling cylinder. The control modes used in the experiment are seven days and 24 hours. During routine operation the Seven Days Mode was applied. At the beginning of each IOP the operation mode was set to 24 hours which yields a temporal resolution of one hour that corresponds to the resolution of the extrapolated AOC and the Rotorod measurements. Tests performed on the pump performance of both types of Burkard traps with a hot-wire flowmeter in the framework of the experiment showed that the air flow rate is 10 l/min with an uncertainty of 5% and is rather stable.

For the pollen counting the sampling strip is divided into sections corresponding to the temporal resolution. This already entails a loss of pollen, since the aperture dimensions and the cylinder rotation cause a 'smearing' of the signal across two subsequent intervals in the proximity of the aperture. The pollen are counted with a microscope in four separate horizontal sweeps along the slide. The total number is then extrapolated to represent the pollen number on the entire slide. The concentration is determined from the pollen counts and the air volume that had passed through the orifice. The statistical significance of the count depends on the

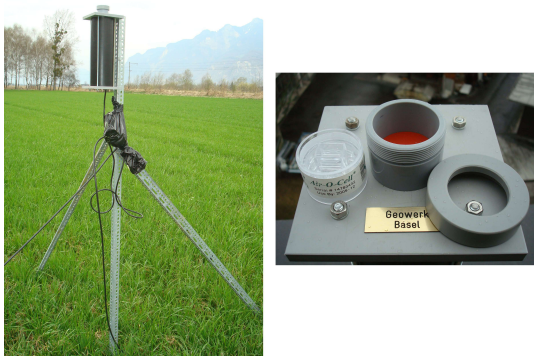

Figure 3.8: Mounting of the AOC pump (left) and AOC cassette and its fixture in the pump (right).

size of the microscope field (i.e. the visible slide area, dependent on the microscope magnification), the number of microscope fields, the applied analysis method (horizontal or vertical lines or random cells) and the number of pollen (see Comtois et al. (1999)).

Air-O-Cell pollen trap

The large number of point measurements for probing horizontal pollen concentration profiles determined the need for alternative, above all cheaper, equipment. AOC volumetric pollen traps (Levetin (2004), Fig. 3.8) also work according to the impaction principle. The AOC itself is a plastic cassette containing a silicone-coated slide below a rectangular orifice which narrows to a slot similar to the Burkard slot. Continuous measurement can only be performed by exchanging the cassettes at the required intervals. A single slide represents the total number of pollen trapped during the sampling period which consequently equals the temporal resolution. The air flow past the slide is provided by a pump, which is hermetically connected to the sampling cassette. Again in terms of saving costs the air pump has been designed and built specially for this experiment according to the manufacturer's recommendations. These imply an air flow rate of 15 l/min to achieve a performance similar to that of the Burkard samplers. In fact, the self-built air pump provides an average air flow rate of 19 l/min. Thus, one could also sample particle sizes in the lower part of the particle weight spectrum. The air flow rate of the self-made pump is 19 l/min with an uncertainty of 5% and is fluctuating rather strong. In opposition to the counting procedure of the Burkard traps, there is no signal 'smearing' and the statistical significance of the pollen count is better, since one slide corresponds exactly to one measuring interval and the entire slide is analyzed.

Rotorod pollen trap

A second, quite different sampling method was applied using Rotorod Model 20 samplers (Sampling Technologies Inc.) (Mandrioli et al., 1998) attached to the tethered balloon for vertical profile measurements of pollen concentration. Basically, this pollen sampler consists of a electric motor which rotates two vertical four-sided

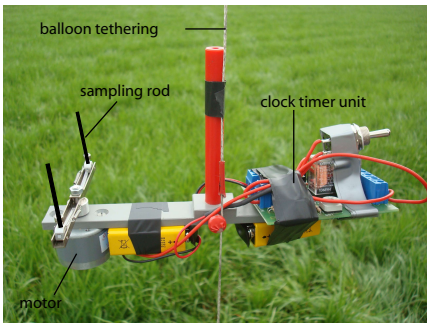

Figure 3.9: Modified Rotorod attached to the balloon tether. The black lines show the position of the sampling rods during operation.

rods (Fig. 3.9). The particular side facing the clockwise rotating direction is coated with silicone. Hence, pollen are trapped as the rods move through the air. From the rectangular area moving ahead and the cyclic distance covered in a certain amount of time, a volume can be determined which corresponds to the sampling volume. The pollen concentration can be calculated via $\frac{n_p}{3.12} = c_p$, where n_p is the absloute number of trapped pollen and c_p is the pollen concentration per cubic meter. The rotation rate is 2400 rpm. It was necessary to modify the original design of the Rotorods to achieve a lower weight and fix them to the tether. The sampling period was one hour to match the temporal resoultion of the other pollen sampling devices used in the experiment. It was crucial to avoid the Rotorods to collect pollen during the ascent (which took 8-10 minutes), since the ascending pollen concentration profiles would be mixed with the measured data during the level period. The fixture of the rods was designed to hold the rods protected from pollen settling when the motor is not operating. A clock timer switched on the Rotorods when the balloon had reached its final position. After one hour of measurement, the sampling was stopped before the balloon was reeled in. The counting procedure was performed equally to the AOC counting method.

3.3 Intercomparison of pollen sampling methods

Among the pollen and spore sampling methodology the volumetric methods earned a preferential position, because the direct information on atmospheric concentrations (e.g. in opposition to absolute particle deposition) is important for near-real-time pollen concentration monitoring in the context of health-impact, as well as the validation of pollen dispersion models. Only a small number of different instrument types exists that are widely used for scientific applications. They all make use of the impaction principle, where airborne particles together with a known volume of air are accelerated relatively to a defined accumulation area. In most cases only a sample of the collected pollen total is counted manually and extrapolated, since the analysis is very time-consuming and impedes real-time results.
The impaction method incorporates errors arising from the physical sampling efficiency (the ratio of collected pollen to the actual pollen number in the considered volume of air) as well as from the counting procedure. Comtois et al. (1999), Aizenberg et al. (2000), Grinshpun et al. (2005) and Gottardini et al. (2009) have

performed laboratory tests on the pollen density distribution among the measuring area of volumetric pollen samplers. They showed that on the one hand the distribution is mostly inhomogeneous and on the other hand that the distribution depends on the pollen size. Comtois et al. (1999) concluded that the mean error found using the standard counting protocols of 4 horizontal lines was approximately 28 %. Only when at least 33.3 % of the slide area was counted a mean error around 10 % was reached. Grinshpun et al. (1994) and Henningson and Ahlberg (1994) have evaluated the physical sampling efficiency of different sampler types. They found sampling efficiencies between 8 and 150 %, depending on the wind velocity and the orientation of the sensor. Upton et al. (1994) performed wind tunnel tests to evaluate effects of sampler inlet design and orientation as well as wind velocity. They showed that the sampling efficiencies vary significantly among the tested different instrument types, which all make use of the impaction principle. The physical sampling efficiency decreased from 100% to 10% with increasing particle diameter (being the most important limiting factor in most cases).
Although the instruments are widely used, only few quantitative information on their uncertainty is found in the literature. Banks and Di Giovanni (1994), Levetin (2004) and Heffer et al. (2005) have performed comparisons of different pollen sampler types. They showed that the deviations can range up to more than 200 percent depending on the compared instrument types.
Prior to and after the main experiment in April, two pollen sampler intercomparisons have been conducted at two different locations. Their aim was to provide information on the precision of AOCs and Rotorods and on their relative agreement to the Burkard sampler, which was used as reference.

The first intercomparison has been conducted in Zurich on March 1^{st} 2009 prior to the main experiment. The targeted pollen species was hazel (*Corylus avellana*), their pollination season ranges from the end of January to the begin of April. The instruments were located on the roof of the MeteoSwiss building in approximately 15 m height above the ground on a hill slope in a suburban area. This is an operational site and not directly influenced by local pollen sources. The set-up consisted of an AOC system, which was mounted on a tripod and the operational Burkard sampler, which was used as reference (Fig. 3.10). All instruments were operated simultaneously around noon on three subsequent intervals of one hour each.
The second intercomparison has been conducted at Locarno-Monti from July 8 to 10 after the main experiment. In this case the targeted pollen species was chestnut (*Castanea sativa*), their pollination season ranges from mid-June to mid-August. The intercomparison also took place at an operational MeteoSwiss site, which is not directly influenced by local pollen sources. The instruments were mounted on the roof of the MeteoSwiss building at a height of approximately 10 m above the ground on a hill slope in a suburban area. The instrumentation consisted of two tripods, each carrying an AOC and a Rotorod. They have been mounted next to the operational Burkard sampler which was used as reference (Fig. 3.11).

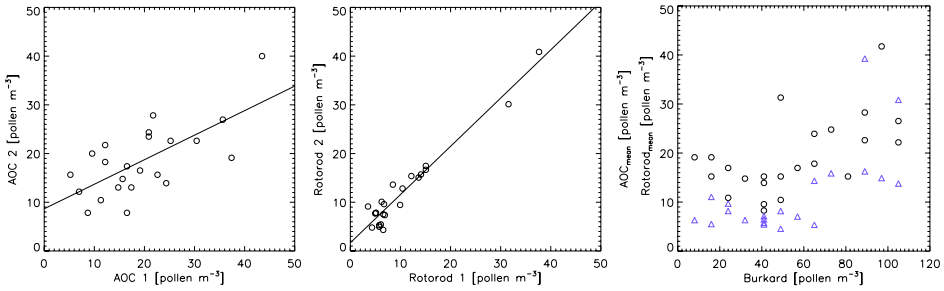

(a) AOC vs. AOC (b) Rotorod vs. Rotorod (c) Burk. vs. AOC/Rotorod

Figure 3.12: Intercorrelation of pollen data measured in Locarno-Monti with a) 2 AOCs; b) 2 Rotorods; c) Burkard and 2 AOCs averaged (circles) and 2 Rotorods averaged (triangles), respectively.

Figure 3.10: Set-up of intercomparative measurements in Zurich. On the left the Burkard Sc. and on the right the AOC system is displayed.

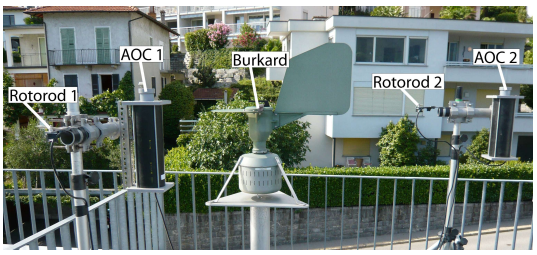

Figure 3.11: Set-up of intercomparative measurements in Locarno-Monti. The permanently installed Burkard pollen sampler was located between two identical mobile AOC and Rotorod supports.

Table 3.3: Comparison of Burkard and AOC pollen measurements in Zurich on March 1^{st}. The time is given in UTC+1

time interval	Burkard	AOC	
12:00 - 13:00	16	30	pollen m^{-3}
13:00 - 14:00	24.31	10	pollen m^{-3}
14:00 - 15:00	24.31	24	pollen m^{-3}

In Table 3.3 the pollen concentrations measured in Zurich in March with a Burkard and an AOC are compared. The absolute number of sampled pollen as well as of the sampling intervals is small. Thus, the significance of these figures is rather low (Comtois et al., 1999).
Figure 3.12 shows the data reproducability of AOC and Rotorod samplers as well as the agreement of the different sampler types to each other. It indicates a rather good precision of the (a) AOC and (b) Rotorod samplers. Figure 3.12c shows, however, that there are significant differences between all instrument types. Although the Burkard sampling method is considered as the reference, it is remarkable that

the AOC and Rotorod methods agree considerably better. Since the Burkard and AOC methods make use of the identical sampling principle and are similar in design, one would rather expect them to show smaller deviations, than AOC compared to Rotorods, which use completely different sampling methods.

Overall, the dicrepancies in the pollen reading between the different instrument types are too substantial to be neglected. Yet the number of data points obtained from the intercomparisons is too small to derive robust estimates for relative calibration coefficients and necessarily different pollen types were used in the intercomparison experiments. During the birch pollination season 2010, therefore, a third pollen sampler intercomparison study was performed using birch pollen. The gained data should provide the information to devise a relative calibration for the pollen observations made in 2009.

4 Data availability

Figure B.1 gives an overview of the data availability for the whole measurement period and all the operated instruments. Note that some instruments measured several different variables.
During the whole first IOP on April 9 and a large part of the second on April 10 data from all Burkard pollen traps are missing due to operation errors. On April 10 there are no available data from the Burkard Sc. samplers, because of instrumental power failures. The two large data gaps of the Burkard T_3 at 18 m from April 12 to 14 and on April 16 occurred because of operation errors. The Rotorod on the balloon tether at 25 m above the ground stopped working on April 13 and was not replaced. The rigging of the balloon sonde broke during the foehn event on April 10 (see Section 5.1.2) and the windvane was lost. Hence the wind direction measurement failed for the rest of the campaign.
The measurements of the five sonic anemometers on T_2 and all the measurements performed at the meteorological station (including the two psychrometers mounted on T_2) provided a data availability of 100 percent. T_1 was removed before the end of the experiment upon landowner request. There was a power failure on April 16 in the evening, which lead to missing data from the tower T_3 and the SODAR. The data availability of the SODAR also depends on the backscatter signal received from atmospheric layers. Figure 4.1 shows the percentage of data availability as function of height. With a vertical resolution of 10 m the measurements reached from 30 to 600 m above the ground. Generally, the vertical data availability was larger than 95 percent for heights between 30 and 300 m. At T_3 some shorter periods of missing data occurred due to software problems with the CR1000 data logger, which was replaced on April 13. However, it turned out that the CR1000 can not properly process simultaneous operation of three ultrasonic anemometers at a sampling rate of 20 Hz, resulting in occasional output errors of raw and flux data at both towers T_1 and T_3. On April 20, the sampling rate of the ultrasonic anemometers was set to 10 Hz for the three remaining days of the campaign.

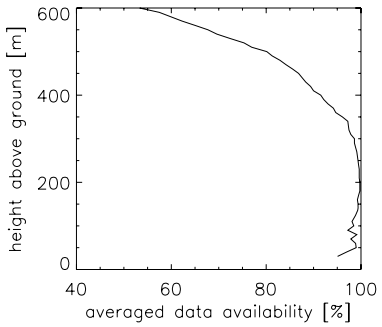

Figure 4.1: Height dependent SODAR data availability.

5 Plausibility and characteristics of meteorological and pollen data

Note that it is not the scope of this experimental report to describe and analyze the results of the meteorological and pollen concentration measurements in detail. Rather we present subsets of the data to give an indication for the plausibilty and variability as well as the characteristics of the measurements. The detailed analysis and discussion of the measured data will be the subject in future works.

5.1 Meteorological conditions

The meteorological conditions during the experimental period can be considered ideal. The weather was fair throughout most of the time and precipitation was measured on two subsequent days only. This is important, because pollen are not released and washed out of the atmosphere during precipitation events. During clear weather periods the solar radiation induced a distinct mountain-plains wind system, which was mostly decoupled from meso-scale systems.

5.1.1 Global radiation and air temperature

According to the ample experience at MeteoSwiss in long-term pollen monitoring the air temperature generally was high enough during the day to allow pollen release (more than approximately 8 degrees C). The mountain-plains wind system behaved as expected, i.e. the wind direction changed from diurnal upvalley to nocturnal downvalley winds almost every diurnal cycle.
Figure 5.1 shows the diurnal course of radiation and dry temperature at two heights. The shortwave downward radiation (rsd) indicates that in the first half of the experiment period the cloudliness was clearly lower than in the second half. Nonetheless, rsd was rather high throughout the entire experiment (with daily maxima around 800 W m^{-2}). The clear weather period during the first half of the experiment was characterized by increasing daily air temperature means due to the strong surface heating. There was a distinct interruption of the clear weather period from April 16 to 20 due to a cold front passage. Shortwave downward radiation and air tem-

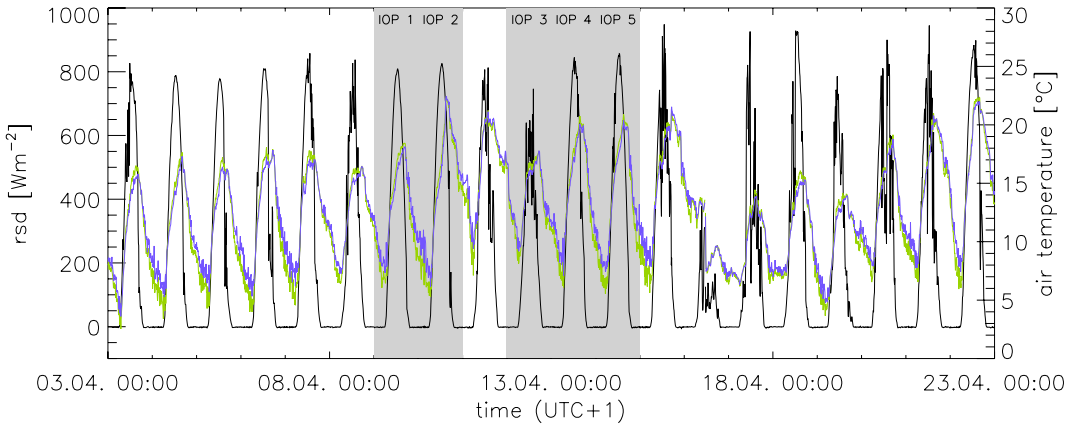

Figure 5.1: 10 min averaged shortwave downward radiation (rsd) and dry air temperature at 2 m (green) and 6.5 m (blue) during the experiment. Shortwave downward radiation (black line, left ordinate) and temperature (blue line, right ordinate) at 2 m above the ground.

perature then decreased significantly. The front passage is the only period where precipitation was detected (with a total amount of 3.9 mm). On the subsequent days until the end of the experiment on April 24 solar radiation and air temperature again increased.

5.1.2 Wind conditions

The wind conditions during the experiment, i.e. the wind direction and velocity, are of special interest, because the experimental design required specific conditions, as mentioned earlier. In addition to the wind measurements using ultrasonic anemometers (see Section 3.2.2) the data of the SMN station at Aigle are presented. The SMN sation is located centrally in the Rhone Valley 3.11 km north of the experimental site (Fig. 3.1). The surrounding area in the centre of the Rhone valley is free of obstacles and, therefore, undisturbed. The station thus represents the synoptic meteorological conditions of the northern valley region. The horizontal wind vectors were measured using a rotating propeller anemometer at 10 m above the ground. The spatially separated measurements give an indication of the difference between regional and local conditions at the experiment site.

Wind direction

Figure 5.2 presents the wind directions measured during six days covering all five IOPs at the three towers at 9 m and at the SMN station at 10 m above the ground. The wind direction measured at the SMN station (orange line) is compared to the experimental measurements 30 m north (black line), 100 m south (green line) and 350 m south (blue line) of the birch plantation. Note that from April 11 to 13 the data of the latter are missing (Section 4). The figure indicates the existence of a mountain-plains wind system with alternating wind directions in a diurnal cycle. During the periods from approximately 10:00 to 16:00 a clear upvalley wind prevailed, when all sensors measured wind directions between 300 and 360 degrees. The phases

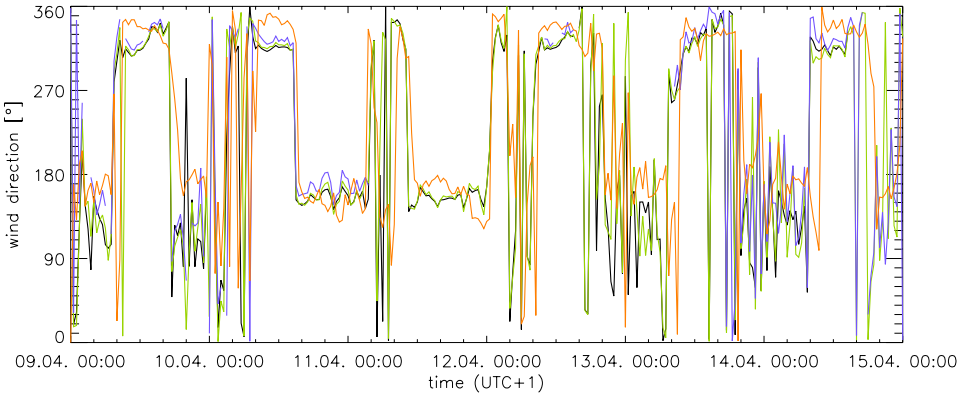

Figure 5.2: Intercomparison of 30 min averaged wind direction measured with a CSAT3 30 m north (black), 100 m south (green) and 350 m south (blue) of the pollen source at 9 m above the ground and at the SMN station in Aigle (orange) at 10 m above the ground.

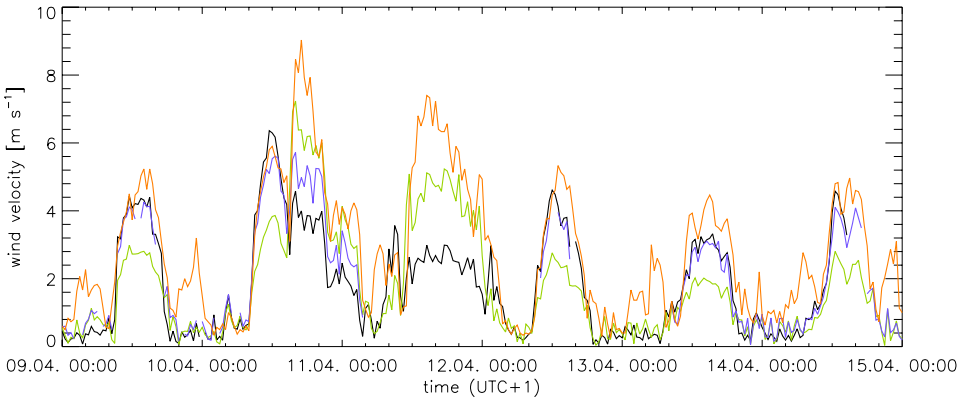

Figure 5.3: Intercomparison of 30 min averaged wind velocity measured with a CSAT3 30 m north (black), 100 m south (green) and 350 m south (blue) of the pollen source at 9 m above the ground and at the SMN station in Aigle (orange) at 10 m above the ground.

between the upvalley wind periods were characterised by strong fluctuations of wind direction, which were also detected by all sensors. Note that the nighttime wind velocities at the experimental site, which will be discussed later, are significantly smaller than during daytime and therefore wind direction measurements are not as robust as during daytime. Yet the nighttime conditions can generally be identified as downvalley winds. The transition phase between up- and downvalley wind is not very distinct in the case of the sonic measurements.

5.1.3 Wind velocity

Figure 5.3 shows the 30 minutes averaged wind velocities corresponding to Fig. 5.2. The mountain-plains system cycles are represented by subsequent periods of alternately higher and lower average levels of wind velocities, whereas the higher levels correspond to the upvalley wind and the lower levels to the downvalley winds. There

is a clear diurnal pattern of the wind velocity during the displayed period. On April 10 and 11, however, higher velocities were measured. These occurrences denote an observed south foehn with significantly increased wind velocities.
The difference between the locations is significantly larger than in te case of wind direction, because the roughness elements at the experimental site have a greater impact on wind velocity than on averaged direction. Only the day- and nighttime upwind fetches of the SMN station are free of obstacles. Hence, the highest wind velocities were generally reached at the SMN station (orange line) with daily maximum values between 5 and 5.5 m s^{-1} during the first three, and approximately 6.5 m s^{-1} during the last day of the displayed period. The nighttime maxima reached 2 to 3 m s^{-1} and were also higher than at the other locations. Among the tower measurements at 9 m height, the station 30 m upwind (black line) and 350 m downwind (blue line) of the birch plantation generally measured the highest wind velocities. The daily maxima reached however less than the SMN station, i.e. around 4 on the first three, and 5.5 m s^{-1} on the last day of the plotted period. During the night the sonic measurements agreed well to each other, yet with rather low wind velocities of less than 1 m s^{-1}. Comparing the wind velocities measured at the SMN station and the experimental site indicates that the downvalley wind is approximately half as strong than above rough terrain as above undisturbed terrain. The large and numerous roughness elements found in the upwind region effect a large decrease in wind velocity at all experimental stations. In Appendix A the SODAR measured distribution of wind velocity and direction at 230 m height is presented, and Fig. A.3 presents the SODAR measured vertical distribution of wind velocity velocity up to 600 m height.

An overview of the dicussed wind conditions valid for the IOPs is presented in Fig. 5.4 and 5.5. They display the temporal pattern of wind direction and velocity during all IOPs on a diurnal basis for the SMN station (green rectangles) and 100 m south of the birch plantation (blue triangles). Both figures show that the daytime upvalley wind was very distinct during the IOPs. This indicates that the arrangement of AOCs and Rotorods south of the birch stand was in the right place to cover the essential parts of the expected pollen plume.
The correlation of low wind velocity to fluctuation of wind direction, which was mentioned earlier for the measurements at the experimental site, is shown more clearly in Fig. 5.4 and 5.5. The wind direction measured at the SMN station when the velocity was generally higher, is quite persistent compared to the dispersed values at the experimental site, when the velocity was very low. The single branch of wind directions around 180 degrees in Fig. 5.4, which occurred between 15:00 to 22:00 and is seen at both stations consists of subsequent 30 min values during the second IOP on April 10, and denotes the foehn event mentioned earlier. The values of the same period shown in Fig. 5.5 confirm this statement with wind velocities twice as high as the temporal corresponding average level of velocity on the other days.
The wind direction also shows that the upvalley wind was generally developed earlier at the experimental site than at the SMN station.

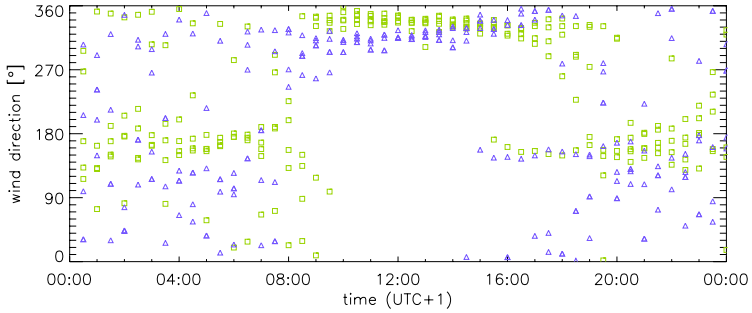

Figure 5.4: Diurnal cycles of wind direction measured at 100 m south of the source at 9 m above the ground (blue triangles) and at the SMN station at 10 m above the ground (green rectangles) during IOPs. 30 min averages are overplotted on a diurnal basis.

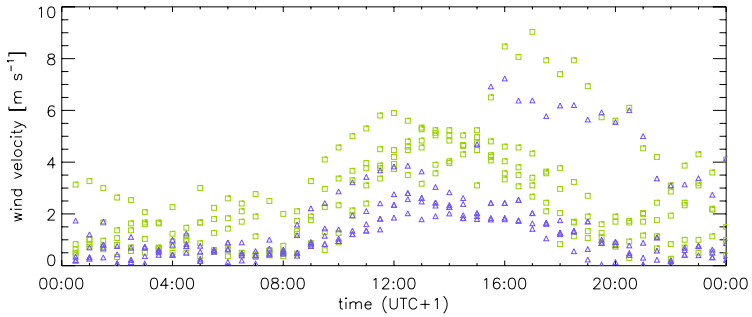

Figure 5.5: Diurnal cycles of wind velocity measured at 100 m south of the source at 9 m above the ground (blue triangles) and at the SMN station at 10 m above the ground (green rectangles) during IOPs. 30 min averages are overplotted on a diurnal basis.

5.1.4 Turbulence intensity

The sonic standard deviation of the vertical velocity component σ_w as a measure of turbulence intensity, normalized to the mean wind velocity $\overline{u}$ yields a dimensionless parameter for turbulence intensity. In Fig. 5.6 it is plotted against $\overline{u}$. The situations at the three towers at 2 m and 18 m height are compared for the periods from 10:00 to 18:00, when upvalley winds prevailed. It is shown that the turbulence intensity was mostly less than 0.5 and exhibits an asymptotic course when plotted against the mean velocity. In the case of 5.6a the turbulence intensity was strongest when the wind velocity was less than 2.5 m s^{-1}. For larger velocities the turbulenc intensity was nearly constant around 0.15. The turbulence intensity near the ground was quite homogeneous throughout the experimental area. Only for wind velocities less than 3 m s^{-1} an effect of the birch plantation could be noticeable, in cases where the turbulence intensity 100 m south of the source (green circles) was larger than upwind (black circles) of the plantation or further downwind (blue circles). 5.6b indicates that the turbulence north and 350 m south of the plantation was weaker at 18 m height than near the ground for the same wind velocities. Yet it is shown clearly that the birch trees induced wake turbulence which yields turbulence intensities larger than 0.2 at the near downwind tower (green circles) for wind velocities less than 5

m s^{-1}. The turbulence intensity 100 m downwind of the plantation and at 2 m was weaker than at 18 m above the ground, possibly because less turbulence was induced in the trunk space than in the leaf area. The data points at wind velocities larger than 5 m s^{-1} in Fig. 5.6b account for the foehn event on April 10 and 11.

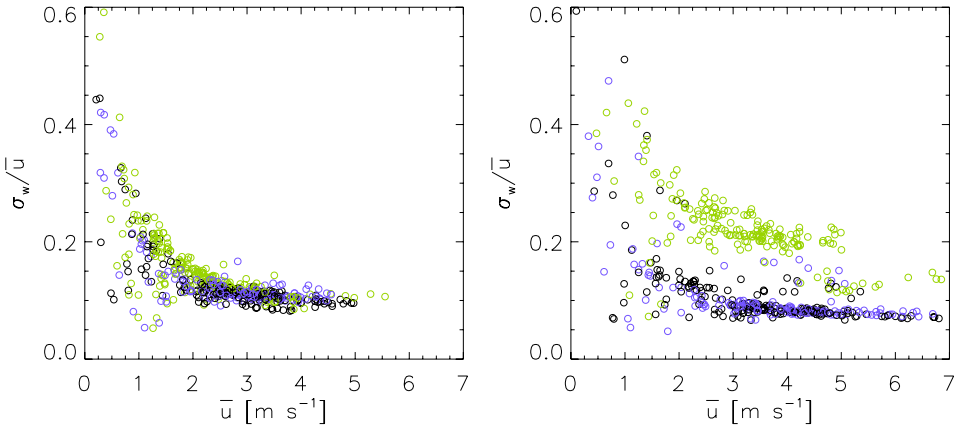

(a) 2 m above the ground

(b) 18 m above the ground

Figure 5.6: Normalized 30 minute average of turbulence intensity measured with CSAT3 at a) 2 m above ground and b) 18 m above ground; 30 m north (black circles), 100 m south (green circles) and 350 m south (blue circles) of the birch plantation. The sampling periods from 10:00 to 18:00 UTC+1 on April 4 to 13 are displayed.

5.2 First assessment of the pollen data

Note that in the case of pollen monitoring the used instrument types apply different methods of pollen sampling. In terms of data comparison the determination of the instrument uncertainties is crucial and a subject of further analysis. At the current state of this work, pollen concentrations are calculated according to the manufacturer's recommendations. This section thus gives an indication of the plausibility and characteristics of the pollen data as well as on the agreement among instruments of the same type. The Burkard pollen traps represent the reference instrument for all pollen concentration measurements conducted in this experiment.
Figure 5.7 shows the course of pollen concentrations during three IOP days measured with Burkards (Sc.) and AOCs. The plot leads to three important statements: First, the dicrepancies between AOC (dashed lines) and Burkard (solid and dotted lines) measurements are significant and, therefore, can only be compared with extensive relative calibration. This is consistent with the findings of the instrument intercomparison study presented in Section 3.3. These results are, however, at odds with the conclusions of Aizenberg et al. (2000), who compared the performance of Burkard and AOC samplers under labatory conditions. They found a significantly better agreement of the two methods for smaller particles, however. This suggests that the validation of the pollen measurements performed under natural conditions is an important subject of investigation in the process of this project. Each sampling

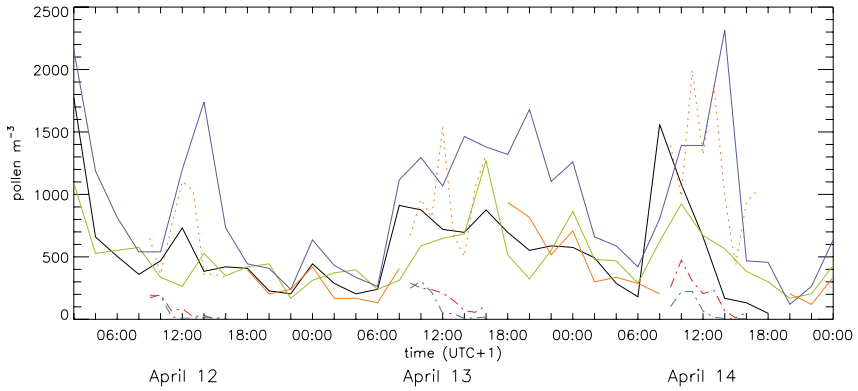

Figure 5.7: Diurnal course of pollen concentrations measured during IOP 3 to 5 at 2 m above the ground. Solid lines denote 2-hourly resolution, dashed and dotted lines denote 1-hourly resolution. Burkard data from 30 m north (black), 30 m south (green), 100 m south (orange) and 350 m south (purple) of the source shown. The dashed orange line denotes Burkard Sc data. AOC data from 100 m south (red) and 200 m south (light blue) of the source are shown. The lines denote the spatial average of the two AOCs adjacent to the corresponding Burkard trap (Fig. 3.4). A data point corresponds to the end of a 2-hourly or 1-hourly interval, respectively .

method underlies uncertainties that are involved in the counting work as well as in the impaction method, in which inertial effects become effective.
Therefore, detailed intercomparison of the different sensor types and relative calibration among the instruments in the field is urgently needed before firm statements about the spatial distribution of pollen can be made. Second, the pollen concentrations indicate a diurnal cycle with a daytime maximum and a nightime minimum, except for the night before April 12, where very large concentrations were measured. This is consistent with descriptions of the diurnal pollen immission pattern of different plant species (Ogden et al., 1969; Von Wahl and Puls, 1989; Van Hout et al., 2008) and among others for birch pollen (Jäger, 1990; Mahura et al., 2009). Third, the impact of the source on downwind pollen concentrations is visible only at some downwind distance: The daytime concentrations at 350 m distance from the source (solid purple line) exceeded those measured at 30 m (solid green line) and 100 m (solid orange line) downwind of the source, which more or less correspond to the background concentration (solid black line).
In Fig. 5.8 pollen concentrations from only one sensor type (AOC) are compared in the following order to assess instrument consistency and get an indication for spatial variability. The course of lateral and longitudinal pollen concentration downwind of the birch plantation for single intervals averaged over all five IOPs is presented. The data indicate that the day to day variability is larger in the hours of large concentrations and that there is a dicernable spatial variability even when concentrations are low. The pollen concentrations measured from 08:00 to 09:00 (Fig. 5.8b) were never exceeded in the afternoon (not shown here). Hence, according to AOC measurements the most important pollen concentrations at ground level near the source are observed before noon.

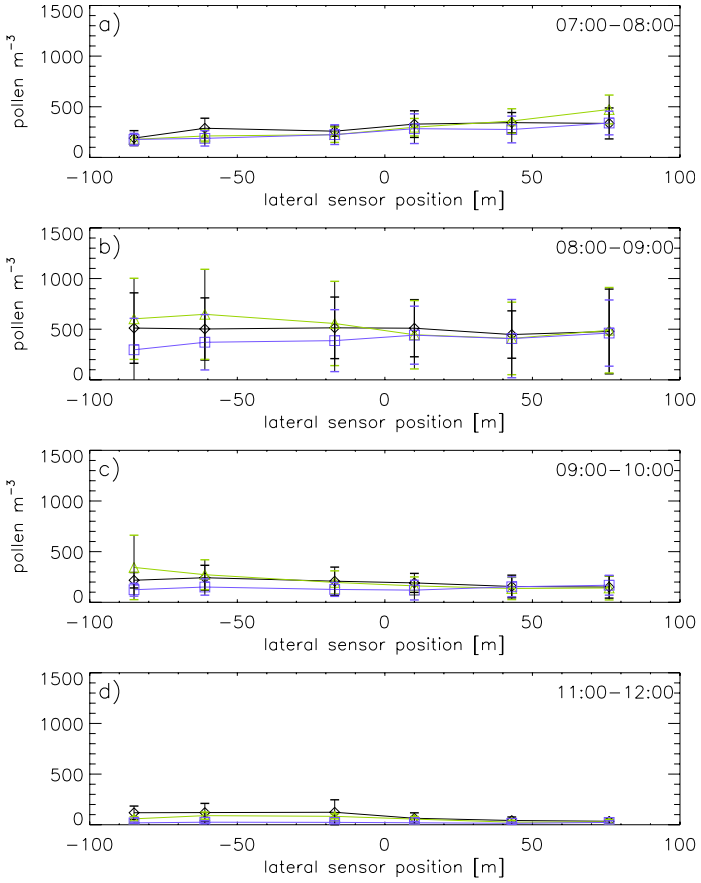

Figure 5.8: Temporal course of lateral and longitudinal birch pollen concentration for corresponding intervals averaged over all five IOPs. The time denoting the end of measurement intervals is UTC+1. The black line denotes the AOC row at 100 m, the green line denotes the AOC row at 200 m and the blue line denotes the AOC row at 350 m downwind of the. The zero value of the abscissa denotes the centre of the pollen source in the lateral direction, positive values account for measurements on the eastern and negative values on the western part of the downwind area. The horizontal lines denote the standard deviation of each AOC for corresponding intervals averaged over all IOPs.

Figure 5.9 shows the vertical pollen concentration profiles measured with Rotorods once or twice in each IOP. It is apparent that the pollen concentration is considerable even at larger heights. The preliminary pollen data, however, do not indicate any systematic profile distribution.

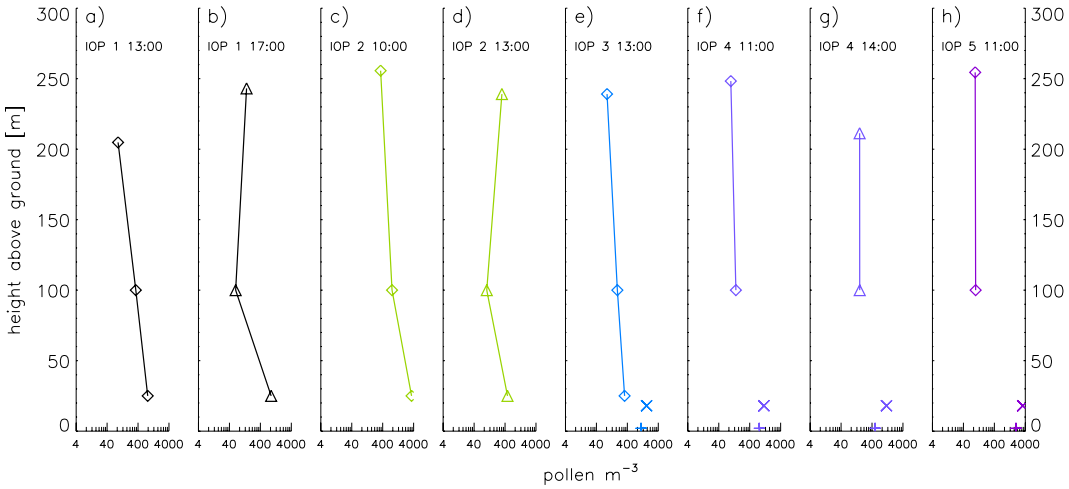

Figure 5.9: Vertical profiles of pollen concentration measured with Rotorods attached to the balloon tether plotted on a logarithmic abscissa. The top profile height is corrected according to the pressure gradient measured with the WXT at 2 m and the meteorological balloon sonde. Burkard Sc. data at 2 m (plus sign) and 18 m (cross) above ground. The time is UTC+1

6 Conclusions

The meteorological measurements during the experiment suggest that the weather conditions coincided with the requirements for probing the downwind pollen concentration emitted by a well-defined source. This is confirmed by the significantly high level of birch pollen concentration. The experimental period can altogether be accounted for a seasonal pollen emission cycle. The existence of a well-defined mountain-plains wind system during most of the experimental period allowed to determine the most appropriate instrumental set-up. The alternating wind direction was cyclically quite persistent. What remains uncertain and still needs to be analized, however, is whether the high spatial and temporal sampling resolution allowed to reliably assign the measured pollen to a known source.
The horizontal pollen profile measurements exhibit significant spatial variations, which have yet to be correlated to micrometeorological factors. The spatial variability during the downvalley wind cycles is substantial and appears to be characteristic if only one sensor type is considered. However, these spatial characteristics are very inconsistent for different pollen sensors. If the Burkard sampler is taken as reference, the AOC and Rotorod samplers generally underestimate the concentrations in the case of several different pollen types. The limited data set of available sensor intercomparison does however not allow for any firm conclusions concerning relative comparability. The large difference of pollen concentrations when applying manufacturers calibration was certainly unexpected at the outset of the experiment and will have major impact on the future progress of data evaluation. The knowledge of the uncertainties and standard variances of each sampling methods is crucial for a significant analysis of the pollen dispersion downwind of the source.

Several (large) gaps in the data series of different instruments impede the analysis of certain periods, i.e. the two first IOPs. The data availability and quality presented and discussed here seem however very promising in terms of eventually leading to a better understanding of pollen emission characteristics, above all the parameterisation of pollen emission and its implementation into operational pollen forecast systems. Furthermore, the large data set collected during this experiment covers a variety of different important micro- and biometeorological parameters of which each could contribute to associated fields of study.
The preliminary results highlight the importance of counting pollen probes in-situ to optain an indication of the plausibility of pollen data before the end of the experiment. It is also important to perform a regular checking of the pollen samplers, since they are rather prone to malfunctions than electronic devices. Despite the ample experience in measuring meteorological and micrometeorological parameters it turned out that pollen sampling incorporates rather large variabilities due to the statistical evaluation on the one hand and uncertainties in the impaction method on the other hand. Performing a calibration of the used sensors is essential and should be done in the framework of similar experiments.

7 Outlook

The most critical issue in the current work is the relative calibration of the different pollen sampling methods. For this reason, several measuring intervals of the reference instrument (Burkard trap) are revised and statistically analyzed. The slides are re-counted, performing 30 sweeps instead of only four, to enhance the statistical significance of the extrapolated interval concentration. The first results show that the density of the trapped pollen on the sampling strip is not homogeneous. Thus, the number of sweeps may need to be increased for a better statistical evaluation of the pollen number.
In spring 2010 a third intercomparison experiment has been conducted at the experimental site in Illarsaz. The three sampler types used in the main experiment (Burkard, AOC and Rotorod), have been tested against each other under similar meteorological conditions and also with birch pollen. Additionally, the effects of the AOC sensor orientation (i.e. horizontal and vertical) will be investigated. The data of this intercomparison should provide more information about the uncertainties of the samplers compared to each other.

A Meteorological conditions

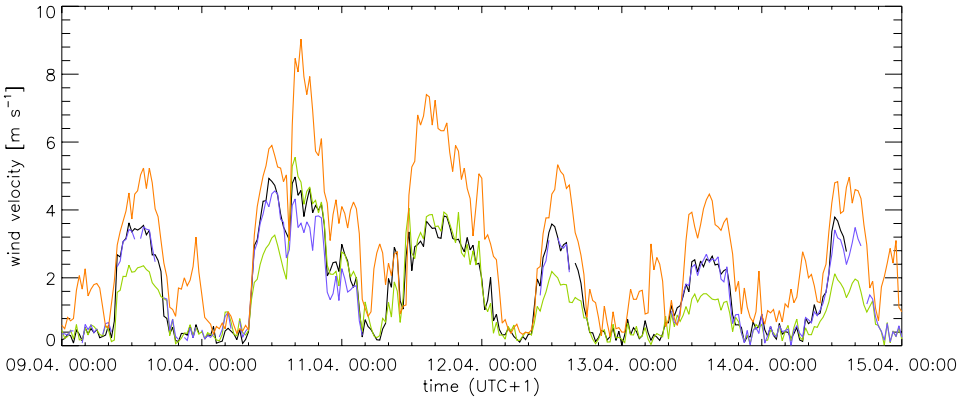

Figure A.1: Intercomparison of 30 min averaged wind velocity measured with a CSAT3 30 m north (black) 100 m south (green) and 350 m south (blue) of the pollen source at 2 m above the ground and at the SwissMetNet station in Aigle (orange) at 10 m above the ground.

Figure A.1 displays the same sampling period as shown in Fig. 5.3 but at 2 m above the ground, which corresponds to the height where ground pollen concentrations have been measured. As expected, it indicates that the wind velocity is generally smaller near the ground. It is also shown that the wind velocity is significantly larger at the SMN station, where the fetch is free of obstacles. Figure A.2 shows the

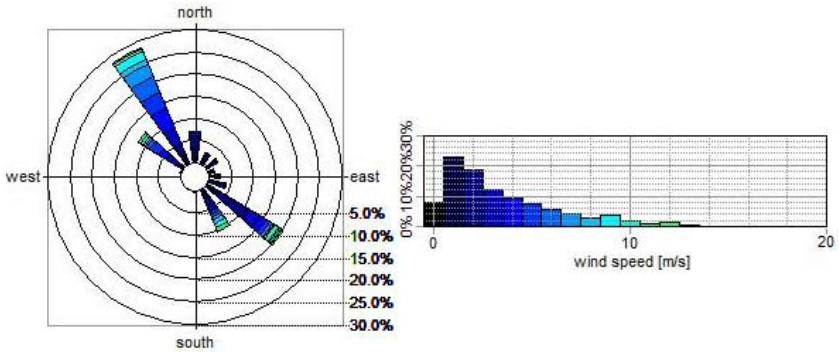

Figure A.2: SODAR measured distribution of wind velocity and direction at 230 m above the ground averaged over the entire measurement period.

wind distribution of wind velocity and direction at 230 m height measured with the SODAR. It indicates that also the elevated wind direction measured at the experimental site corresponds to the results shown in Section 5.1, i.e. the main directions are northeast and southwest, respectively. Hence the data presented here also mostly denote the plains-valley system. A possible superimposition by meso-scale systems can not be identified.

The maximum wind velocity of around 12 m s^{-1} is approximately twice the maximum measured at the SMN station at 9 m height. Approximately 50 percent of

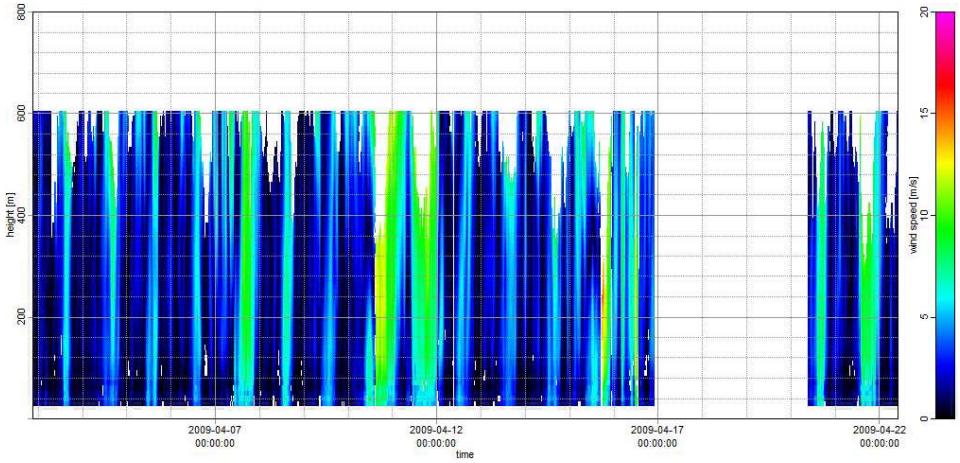

Figure A.3: SODAR measured vertical distribution of wind velocity during the entire measurement period. The spatial resolution is 10 m, the time is given in UTC+1.

the entire data series ranges between zero and 2 m s^{-1}. Figure A.3 indicates that the vertical wind velocity was quite homogeneous up to 230 m height. The two occurrences on April 10 and 11 with wind velocities of around 10 m s−1 throughout most of the probed distance denote the foehn events mentioned earlier. The reasons for the data gap from April 16 to 20 are mentioned in Section 4.

B Data availability

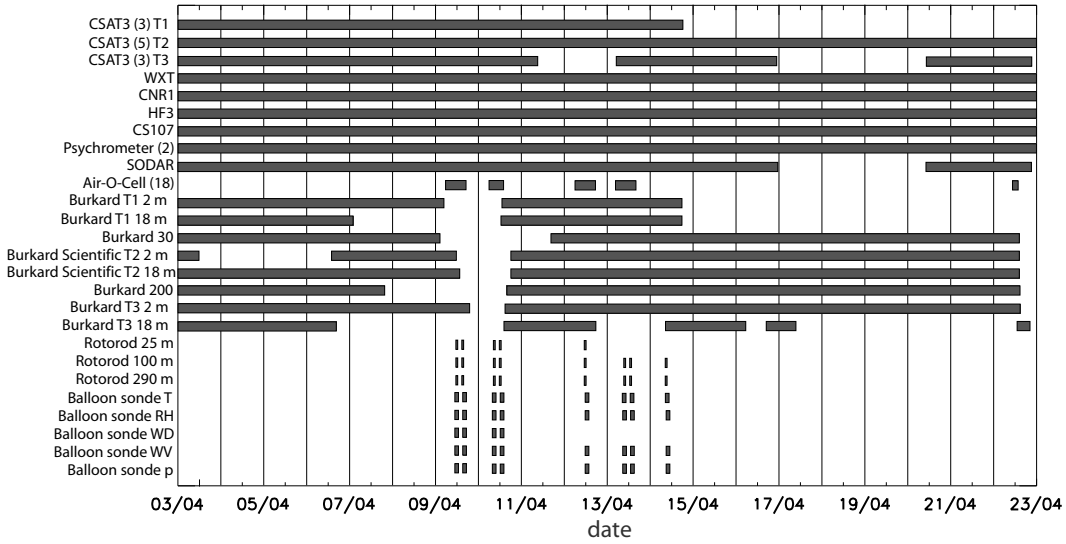

Figure B.1: Data availability for the whole measurement period. The position of the date denotes 00:00 UTC+1. Available data are indicated with the dark grey bar, periods without available data are left blank. Burkard 30 and 200 denote the Burkards located at a distance of 30 and 200 m, respectively, from the birch plantation. T denotes dry air temperature, RH denotes relative humidity, WD denotes wind direction, WV denotes wind velocity, p denotes air pressure.

The most important data gaps presented in the figure concerned the Burkard measurements during the first two IOPs. The AOC operation on April 22 denotes a tracer experiment that has been conducted in terms of validating AOC measurements. A known amount of glass beads the approximate size and weight of birch pollen has been released by hand from a dispenser at 5 m height during the upvalley wind phase. Backwards modeling of the sampled dispersion of pollen concentrations should then be compared to the known effective emission rate. However, because of insufficient release height and clustering effects, a large fraction of the glass beads could not be transported by the wind and settled in the proximate area. Therefore, the subject unfortunately had to be dropped.

Bibliography

Aizenberg, V., Reponen, T., Grinshpun, S. and Willeke, K. (2000), 'Performance of Air-O-Cell, Burkard and Button Samplers for total enumeration of airborne spores', *American Industrial Hygiene Association* **61**, 855864.

Ambelas Skjøth, C., Brandt, J., Christensen, J., Løf strøm, P., Frohn, L., Geels, C., Hvidberg, M., Frydendall, J. and Hansen, K. (2006), THOR: An operational and integrated model system for air pollution and pollen forecasts, *in* 'Proceedings of 8th International Congress on Aerobiology, "Towards a comprehensive vision"', Neuchâtel, Switzerland, 21-25 August 2006.

Arya, S. (2001), *Introduction to micrometeorology*, Academic press, London, United Kingdom.

Aylor, D., Boehm, M. and Shields, E. (2006), 'Quantifying aerial concentrations of maize pollen in the atmospheric surface layer using remote-piloted airplanes and lagrangian stochastic modeling', *Journal of Applied Meteorology and Climatology* **45**(7), 1003–1015.

Banks, L. and Di Giovanni, F. (1994), 'A wind tunnel comparison of the Rotorod and Samplair pollen samplers', *Aerobiologia* **10**, 141–145.

Boehm, M., Aylor, D. and Shields, E. (2008), 'Maize pollen dispersal under convective conditions', *J. of App. Meteorology and Climatology* **47**, 291–307.

Brunet, Y., Foueillassar, X., Audran, A., Garrigou, D. and Dayau, S. (2004), 'Evidence for long-range transport of viable maize pollen.', *Preprints, 16th Conf. on Biometeorology and Aerobiology, Vancouver BC, Canada, Amer. Meteor. Soc. CD-ROM, P4A.2* .

Chamecki, M., Meneveau, C. and Parlange, M. (2009), 'Large eddy simulation of pollen transport in the atmospheric boundary layer', *Aerosol Science* **40**, 241–255.

Comtois, P., Alcazar, P. and Neron, D. (1999), 'Pollen counts statistics and its relevance to precision', *Aerobiologia* **15**, 19–28.

Comtois, P., Fernández-Gonzales, D., Valencia-Barrera, R., Sánchez, J., Fraile, R. and Rodier, S. (2000), 'Pollen content study of the lower atmosphere in León (Spain) by use of a tethered balloon', *Aerobiologia* **16**, 187–191.

De Haan, P. and Rotach, M. (1998), 'A novel approach to atmospheric dispersion modelling: The Puff-Particle-Model', *Quarterly Journal of the Royal Meteorolo-*

gical Society **124**, 2771–2792.

Doms, G. and Schaettler, U. (2002), *The nonhydrostatic limited-area model LM - Part I: Dynamics and Numerics*, Scientific Documentation, Deutscher Wetterdienst, Offenbach, Germany. (available from http://www.cosmo-model.org).

Foken, T. (2008), *Micrometeorology*, Springer-Verlag, Berlin Heidelberg.

Galán, C., Cariñanos, P., García-Mozo, H., Alcázar, P. and Domínguez-Vilches, E. (2001), 'Model for forecasting Olea europea L. airborne pollen in South-West Andalusia, Spain', *Int. J. Biometeorol.* **45**, 59–63.

Gottardini, E., Cristofolini, F., Cristofori, A., Vannini, A. and Ferretti, M. (2009), 'Sampling bias and sampling errors in pollen counting in aerobiological monitoring in Italy', *Journal of Environmental Monitoring* **11**, 751755.

Grinshpun, S., Chang, C.-W., Nevalainen, A. and Willeke, K. (1994), 'Inlet characteristics of bioaerosol samplers', *Journal of Aerosol Science* **25**(8), 1503–1522.

Grinshpun, S., G., M., Trunov, M., Gorny, R., Sivasubramani, S., Adhikari, A. and Reponen, T. (2005), 'Collection of airborne spores by circular single-stage impactors with small jet-to-plate distance', *Aerosol Science* **36**, 575591.

Heffer, M., Ratz, J., Miller, J. and Day, J. (2005), 'Comparison of the Rotorod to other air samplers for the determination of Ambrosia artemisiifolia pollen concentrations conducted in the Environmental Exposure Unit', *Aerobiologia* **21**, 233239.

Helbig, N., Vogel, B., Vogel, H. and Fiedler, F. (2004), 'Numerical modelling of pollen dispersion on the regional scale', *Aerobiologia* **3**, 3–19.

Henningson, E. and Ahlberg, M. (1994), 'Evaluation of microbiological aerosol samplers: A review', *Journal of Aerosol Science* **25**(8), 1459–1492.

Hirst, J. (1952), 'An automatic volumetric spore trap', *Ann. Appl. Biol.* **39**, 257–265.

Isard, S., Russo, J. and Ariatti, A. (2007), 'Aerial transport of soybean rust spores into the Ohio river valley during September 2006', *Aerobiologia* **23**, 271–282.

Jäger, S. (1990), 'Tageszeitliche Verteilung und langjährige Trends bei allergiekompetenten Pollen', *Allergologie* **13**(5), 159–182.

Kaimal, J. and Finnigan, J. (1994), *Atmospheric boundary layer flows: their structure and measurement*, Oxford University Press, Oxford, United Kingdom.

Lavigne, C., Godelle, B., Reboud, X. and Gouyon, P. (1996), 'A method to determine the mean pollen dispersal of individual plants growing within large pollen source', *Theor. Appl. Genet.* **93**, 1319–1326.

Lavigne, C., Klein, E., Vallée, P., Pierre, J., Godelle, B. and Renard, M. (1998), 'A pollen-dispersal experiment with transgenic oilseed rape. Estimation of the average pollen dispersal of an individual plant within a field', *Theor. Appl. Genet.* **96**, 886–896.

Lee, X. (2004), *Handbook of micrometeorology*, Kluwer Academic Publishers, Dordrecht, The Netherlands.

Levetin, E. (2004), 'Methods for aeroallergen sampling', *Current Allergy and Asthma Reports* **4**, 376–383.

Magarey, R. and Isard, S. (2005), Model and dispersal for Asian soybean rust, *in* 'Proceedings of Illinois Crop protection Technology Conference', University of Illinois at Urbana-Campaign, pp. 21–22.

Mahura, A., Baklanov, A. and Korsholm, U. (2009), 'Parameterization of the birch pollen diurnal cycle', *Aerobiologia* **25**, 203–208.

Mandrioli, P., Comtois, P. and Levizzani, V. (1998), *Methods in aerobiology*, Pitagora Editrice, Bologna, Italy.

Masanari, S. and Tadashi, K. (2003), 'Development of automatic pollen monitor and its performance', *Papers of Technical Meeting on Micromachine and Sensor System, IEE Japan* .

Méndez, J., Comtois, P. and Iglesias, I. (2005), 'Betula pollen: One of the most important aeroallergens in Ourense, Spain', *Aerobiologia* **21**, 115–123.

Michel, D., Philipona, R., Ruckstuhl, C. and Vuilleumier, L. (2008), 'Performance and uncertainty of CNR1 net radiometers during a one year field comparison', *Journal of Atmospheric and Oceanic Technology* **25**(3), 442–451.

Nieddu, G., Chessa, I., Canu, A., Pellizzaro, G., Sirca, C. and Vargiu, G. (1997), 'Pollen emission from olive trees and concentrations of airborne pollen in an urban area of North Sardinia', *Aerobiologia* **13**, 235–242.

Ogden, E., Hayes, J. and Raynor, G. (1969), 'Diurnal patterns of pollen emission in Ambrosia, Phleum, Zea and Ricinus', *Amer. J. Bot.* **56**(1), 16–21.

Raynor, G., Ogden, E. and Hayes, J. (1970), 'Dispersion and deposition of Ragweed

pollen from experimental sources', *Journal of Applied Meteorology and Climatology* **9**, 885–895.

Ronneberger, O. (2007), 3D Invariants for automated pollen recognition, PhD thesis, Fakultät für Angewandte Wissenschaften der Albert-Ludwigs-Universität Freiburg im Breisgau.

Rotach, M., Gryning, S. and Tassone, C. (1996), 'A two-dimensional lagrangian stochastic dispersion model for daytime conditions', *Quarterly Journal of the Royal Meteorological Society* **122**(530), 367–389.

Schueler, S. and Schlünzen, K. (2006), 'Modeling of oak pollen dispersal on the landscape level with a mesoscale atmospheric model', *Environ. Model Assess* **11**, 179–194.

Shigeto, K., Toshio, F., Kazuhito, M. and Hiroyuki, S. (2004), 'Development of an automatic corn pollen monitor', *Japanese Journal of Palynology* **50**, 5–14.

Shigetoshi, Y., Tadao, E. and Akira, S. (2005), 'A comparative study between real time monitor KH-3000 and conventional Durham sampler measuring airborne pollen', *Nippon Jibiinkoka Gakkai Kaiho* **108**, 801–805.

Sofiev, M., Siljamo, P., Ranta, H. and Rantio-Lehtimäki, A. (2006a), 'Towards numerical forecasting of long-range air transport of birch pollen: theoretical considerations and a feasability study', *Int. J. Biometeorol.* **50**, 392–402.

Sofiev, M., Siljamo, P., Valkama, I., Ilvonen, M. and Kukkonen, J. (2006b), 'A dispersion modelling system SI-LAM and its evaluation against ETEX data', *Atmosph. Environ.* **40**, 674–685.

Steinacker, R. (1984), 'Areaheight distribution of a valley and its relation to the valley wind', *Contrib. Atmos. Phys.* **57**, 64–71.

Stull, R. (1988), *An introduction to Boundary Layer Meteorology*, Kluwer Academic Publishers, Dordrecht, The Netherlands.

Takahashi, Y., Kawashima, S. and Fujita, T. (2001), 'Comparison between real-time pollen monitor KH-3000 and Burkard sampler', *Arerugi* **50**, 1136–42.

Upton, S., Mark, D., Douglass, E., Hall, D. and Griffiths, W. (1994), 'A wind tunnel evaluation of the physical sampling efficiencies of three bioaerosol samplers', *Journal of Aerosol Science* **25**(8), 1493–1501.

Van Hout, R., Chamecki, M., Brush, G., Katz, J. and Parlange, M. (2008), 'The

influence of local meteorological conditions on the circadian rhythm of corn (Zea mays L.) pollen emission', *Agricultural and Forest Meteorology* **148**, 1078–1092.

Venkatram, A. and Wyyngaard, J. (1988), *Lectures on air pollution modeling*, American Meteorological Society, Boston.

Vogt, R. (1995), Theorie, Technik und Analyse der experimentellen Flussbestimmung am Beispiel des Hartheimer Kieferwaldes., PhD thesis, Stratus, Basel.

Von Wahl, P.-G. and Puls, K. E. (1989), 'The emission of mugwort pollen (Artemisia vulgaris L.) and its flight in the air', *Aerobiologia* **5**, 55–63.

Weigel, A., Chow, F., Rotach, M., Street, R. and Xue, M. (2006), 'High-resolution Large-Eddy Simulations of flow in a steep alpine valley. Part II: Flow structure and heat budgets', *Journal of Applied Meteorology and Climatology* **45**, 87–107.

Arbeitsberichte der MeteoSchweiz

229 Philipona R, Levrat G, Romanens G, Jeannet P, Ruffieux D and Calpini B, 2009: Transition from VIZ / Sippicanto ROTRONIC - A new humidity sensor for the SWISS SRS 400 Radiosonde, 37pp, CHF 66.-

228 MeteoSchweiz: 2009, Klimabericht Kanton Graubünden, 40pp, nur als .pdf erhältlich

227 MeteoSchweiz, 2009, Basisanalysen ausgewählter klimatologischer Parameter am Standort KKWLeibstadt, 135pp, CHF 88.-

226 MeteoSchweiz, 2009, Basisanalysen ausgewählter klimatologischer Parameter am Standort KKW Mühleberg, 136pp, CHF 88.-

225 MeteoSchweiz, 2009, Basisanalysen ausgewählter klimatologischer Parameter am Standort KKW Gösgen, 136 pp, CHF 88.-

224 MeteoSchweiz, 2009, Basisanalysen ausgewählter klimatologischer Parameter am Standort KKW Beznau, 135pp, CHF 88.-

223 Dürr B: 2008, Automatisiertes Verfahren zur Bestimmung von Föhn in den Alpentälern, 22pp, CHF 62.-

222 Schmutz C, Arpagaus M, Clementi L, Frei C, Fukutome S, Germann U, Liniger M und Schacher F: 2008, Meteorologische Ereignisanalyse des Hochwassers 8. bis 9. August 2007, 29pp, CHF 64.-

221 Frei C, Germann U, Fukutome S und Liniger M: 2008, Möglichkeiten und Grenzen der Niederschlagsanalysen zum Hochwasser 2005, 19pp, CHF 62.-

220 Ambühl J: 2008, Optimization of Warning Systems based on Economic Criteria, 79pp, CHF 75.-

219 Ceppi P, Della-Marta PM and Appenzeller C: 2008, Extreme Value Analysis of Wind Observations over Switzerland, 43pp, CHF 67.-

218 MeteoSchweiz (Hrsg): 2008, Klimaszenarien für die Schweiz – Ein Statusbericht, 50pp, CHF 69.-

217 Begert M: 2008, Die Repräsentativität der Stationen im Swiss National Basic Climatological Network (Swiss NBCN), 40pp, CHF 66.-

216 Della-Marta PM, Mathis H, Frei C, Liniger MA and Appenzeller C: 2007, Extreme wind storms over Europe: Statistical Analyses of ERA-40, 80pp, CHF 75.-

215 Begert M, Seiz G, Foppa N, Schlegel T, Appenzeller C und Müller G: 2007, Die Überführung der klimatologischen Referenzstationen der Schweiz in das Swiss National Climatological Network (Swiss NBCN), 47pp, CHF 68.-

214 Schmucki D und Weigel A: 2006, Saisonale Vorhersage in Tradition und Moderne: Vergleich der "Sommerprognose" des Zürcher Bööggs mit einem dynamischen Klimamodell, 46pp, CHF 68.-

213 Frei C: 2006, Eine Länder übergreifende Niederschlagsanalyse zum August Hochwasser 2005. Ergänzung zu Arbeitsbericht 211, 10pp, CHF 59.-

212 Z'graggen, L: 2006, Die Maximaltemperaturen im Hitzesommer 2003 und Vergleich zu früheren Extremtemperaturen, 74pp, CHF 75.-

211 MeteoSchweiz: 2006, Starkniederschlagsereignis August 2005, 63pp, CHF 72.-

210 Buss S, Jäger E and Schmutz C: 2005: Evaluation of turbulence forecasts with the aLMo, 58pp, CHF 70.–

209 Schmutz C, Schmuki D, Duding O, Rohling S: 2004, Aeronautical Climatological Information Sion LSGS, 77pp, CHF 25.–

Frühere Veröffentlichungen und Arbeitsberichte finden sich unter
www.meteoschweiz.ch » Forschung » Publikationen

Veröffentlichungen der MeteoSchweiz

85 Ambühl, J: 2010, Neural interpretation of ECMWF ensemble predictions, 48pp, CHF 68.-

84 Ambühl, J: 2010, Customer oriented warning systems, 91pp, CHF 78.-

83 Ceppi, P: 2010, Spatial characteristics of gridded Swiss temperature trends: local and large-scale influences, 82pp, CHF 76.-

82 Blanc, P: 2009, Ensemble-based uncertainty prediction for deterministic 2 m temperature forecasts, 90pp, CHF 78.-

81 Erdin R: 2009, Combining rain gauge and radar measurements of a heavy precipitation event over Switzerland: Comparison of geostatistical methods and investigation of important influencing factors, 109pp, CHF 81.-

80 Buzzi M: 2008, Challenges in Operational Numerical Weather Prediction at High Resolution in Complex Terrain, 186pp, CHF 103.-

79 Nowak D: 2008, Radiation and clouds: observations and model calculations for Payerne BSRN site, 101 pp, CHF 80.-

78 Arpagaus M, Rotach M, Ambrosetti P, Ament F, Appenzeller C, Bauer H-S, Bouttier F, Buzzi A, Corazza M, Davolio S, Denhard M, Dorninger M, Fontannaz L, Frick J, Fundel F, Germann U, Gorgas T, Grossi G, Hegg C, Hering A, Jaun S, Keil C, Liniger M, Marsigli C, McTaggart-Cowan R, Montani A, Mylne K, Ranzi R, Richard E, Rossa A, Santos-Muñoz D, Schär C, Seity Y, Staudinger M, Stoll M, Vogt S, Volkert H, Walser A, Wang Y, Werhahn J, Wulfmeyer V, Wunram C and Zappa M: 2009, MAP D-PHASE: Demonstrating forecast capabilities for flood events in the Alpine region. Report of the WWRP Forecast Demonstration Project D-PHASE submitted to the WWRP Scientific Steering Committee, 65pp, CHF 73.-

77 Rossa AM: 2007, MAP-NWS – an Optional EUMETNET Programme in Support of an Optimal Research Programme, 67pp, CHF 73.-

76 Baggenstos D: 2007, Probabilistic verification of operational monthly temperature forecasts, 52pp, CHF 69.-

75 Fikke S, Ronsten G, Heimo A, Kunz S, Ostrozlik M, Persson PE, Sabata J, Wareing B, Wichura B, Chum J, Laakso T, Säntti K and Makkonen L: 2007, COST 727: Atmospheric Icing on Structures Measurements and data collection on icing: State of the Art, 110pp, CHF 83.-

74 Schmutz C, Müller P und Barodte B: 2006, Potenzialabklärung für Public Private Partnership (PPP) bei MeteoSchweiz und armasuisse Immobilien, 82pp, CHF 76.-

73 Scherrer SC: 2006, Interannual climate variability in the European and Alpine region, 132pp, CHF 86.-

72 Mathis H: 2005, Impact of Realistic Greenhouse Gas Forcing on Seasonal Forecast Performance, 80pp, CHF 75.-

71 Leuenberger D: 2005, High-Resolution Radar Rainfall Assimilation: Exploratory Studies with Latent Heat Nudging, 103pp, CHF 81.-

70 Müller G und Viatte P: 2005, The Swiss Contribution to the Global Atmosphere Watch Programme – Achievements of the First Decade and Future Prospects, 112pp, CHF 83.-

69 Müller WA: 2004, Analysis and Prediction of the European Winter Climate, 115pp, CHF 34.

68 Bader S: 2004, Das Schweizer Klima im Trend: Temperatur- und Niederschlagsentwicklung seit 1864, 48pp, CHF 18.-

67 Begert M, Seiz G, Schlegel T, Musa M, Baudraz G und Moesch M: 2003, Homogenisierung von Klimamessreihen der Schweiz und Bestimmung der Normwerte 1961-1990, Schlussbericht des Projektes NORM90, 170pp, CHF 40.-

Frühere Veröffentlichungen und Arbeitsberichte finden sich unter
www.meteoschweiz.ch » Forschung » Publikationen